

Spectrochemical Series of Cobalt(III). An Experiment for High School through College

Adam R. Riordan, Ariane Jansma, Sarah Fleischman, David B. Green, and Douglas R. Mulford*

Department of Chemistry, Pepperdine University, Malibu, CA 90263, Douglas.Mulford@pepperdine.edu

Received July 7, 2004. Accepted September 2, 2004.

Abstract: We present a laboratory project suitable for high school through upper-division college courses that has been designed to allow students to qualitatively investigate or quantitatively generate the spectrochemical series for octahedral cobalt(III) complexes. This experiment is useful for concrete, visual demonstration of the structural and electronic properties of ligand-to-metal bonding. Water, ammonia, nitrite, oxalate, glycinate, ethylenediamine, 1,10-phenanthroline, carbonate, and cyanide are used as ligands to form the cobalt complexes. Each complex has a different color and λ_{max} . This allows students to derive the spectrochemical series by visual inspection or UV–visible spectroscopy. At the high school level, the series can be generated from visual inspection of the colored compounds by use of the transmission color wheel. At the general chemistry level, the series can be generated from spectroscopic data using the λ_{max} of lowest energy. In advanced courses students can calculate crystal field splitting values, Δ_0 , and the ordering of the spectrochemical series can be justified from a metal–ligand interaction point of view.

Introduction

Concepts of bonding and the electronic and orbital interactions and changes that occur upon bonding are often difficult for students at all levels in the chemistry curriculum to grasp. These difficulties, and the resulting misconceptions, have been the subject of many papers [1–14]. The bonding between metals and ligands is most often explained at the general chemistry level through crystal field theory (CFT). (A brief review of CFT is presented in the supporting materials.) In more advanced classes, the more powerful ligand field theory (LFT), which incorporates both CFT and molecular orbital theory, is commonly used. It is often difficult for students to grasp these seemingly abstract theories without concrete evidence.

Electronic and orbital changes occur when a ligand binds to a transition metal. These electronic changes are manifested in the splitting of the metal d orbitals during complex formation and are often macroscopically seen as a change of color from the free metal to the complex. The magnitude of this splitting, designated Δ_0 in an octahedral electronic environment, can be measured spectroscopically and depends upon the size and charge of the metal, the ionic nature of the ligand, and according to LFT, the σ and π donor/acceptor characteristics of the ligand. It is said that a “stronger” ligand field will produce a larger Δ_0 , and when several ligands are compared, the spectrochemical series can be produced.

Because the spectrochemical series is a fundamental topic of inorganic chemistry and provides a link between the qualitative concepts of chemical bonding and the quantum mechanical changes that occur during bond formation in transition metal complexes, it provides the logical experimental foundation and validation for CFT and LFT. Because of its predictive power for a wide range of metal–ligand interactions, many instructors require their students simply to memorize the spectrochemical series. Rarely are students required to generate the series for

themselves, and few experiments exist in the literature which allow students to generate a spectrochemical series for more than a few coordination compounds [15–24]. Not only does the synthesis of metal complexes with direct observation of the concomitant color changes provide a satisfying laboratory experience, but experimental generation and verification of the spectrochemical series results in a much deeper understanding of these concepts.

A rigorous analysis of the spectroscopic data to determine the ligand field splitting parameter demands the use of the Tanabe–Sugano (TS) energy-level diagram specific for the metal–complex geometry under study. Despite this requirement, many formally and informally published experiments ignore the use of TS diagrams in the quantitative determination of Δ_0 or provide the reduced data on relatively simple systems and leave it as an academic process to calculate Δ_0 . This experiment represents the first literature-published example the authors have found that allows for an experimental demonstration of this process.

In the investigation described in this paper, the ordering of ligands into a spectrochemical series in terms of their crystal field strength arises both *visually* (from the color of the complex in solution) and *spectroscopically* (by quantitative measurement of the d-orbital splitting). An advantage of this experiment is that it is scalable for high school through upper-division college levels. For introductory levels, the highly colored complexes that result from varying the identity of the ligand bound to a common metal can be used to generate a spectrochemical series by visual inspection. This provides strong physical evidence for the involved electronic effects. With the wide availability of scanning and diode-array UV–visible spectrophotometers, the ligands can be quantitatively ranked by the lowest energy wavelengths of maximum absorption (λ_{max}). Being a direct function of Δ_0 , the λ_{max} of lowest energy can be used to accurately generate the

spectrochemical series. It should be noted, however, that contrary to some previously published experiments [22, 23, 25] for d^2-d^9 metal complexes, Δ_0 cannot be equated to the λ_{max} of lowest energy but **must** be calculated using a Tanabe-Sugano diagram. In addition, in classes in which metal-to-ligand bonding interactions are discussed in detail, the spectrochemical series can not only be produced, but the ranking of ligands can be justified/explained in terms of ligand-bonding interactions such as σ - and π -acceptor/donor.

In this experiment, an extensive spectrochemical series can easily be produced within the time constraints of a normal laboratory class. To clearly demonstrate the crystal field splitting of a wide variety of ligands, this investigation uses a common metal throughout with a single coordination geometry, and all species contain only a single type of ligand. Cobalt(III) is used because it adopts an octahedral geometry for all compounds synthesized in this experiment. There have been other experiments [15–24] that produced limited or mixed metal series, but these previous experiments are inadequate to clearly demonstrate the electronic and orbital changes that occur when a ligand binds to a transition metal.

This laboratory investigation utilizes adapted time-efficient synthetic procedures allowing students to gain both a clearer understanding of the origin of color in certain molecular species and of the structure and bonding information these colors can provide. In addition, these syntheses can be used as a vehicle to discuss many aspects of coordination chemistry including synthesis, equilibrium interactions, solvation effects, formation constants, LeChâtelier's principle, coupled reactions, and redox chemistry.

Experimental

All solutions are analyzed *in situ* so isolation of the solid complexes is not necessary. Though some of these synthetic procedures have been known for some time [26], they have been altered in the current experiment to facilitate completion in a standard three-hour laboratory session. If necessary, syntheses can be spread over more than a single laboratory period.

Hazards. Cobalt(II) nitrate hexahydrate ($\text{Co}(\text{NO}_3)_2 \cdot 6 \text{H}_2\text{O}$) [CAS 10026-22-9] and cobalt(II) chloride hexahydrate ($\text{CoCl}_2 \cdot 6 \text{H}_2\text{O}$) [CAS 7791-13-1]: Contact with cobalt solutions should be treated by washing with soap and water. Chronic exposure to the cobalt ion and its compounds can result in decreased pulmonary function, contact sensitivity and dermatitis, and respiratory distress. $\text{Co}(\text{NO}_3)_2 \cdot 6 \text{H}_2\text{O}$ is an oxidizer; contact with strong reducing agents should be avoided.

Ethylendiammine [CAS 000107-15-3] is harmful if swallowed, inhaled, or absorbed through the skin. The pure liquid has a strong odor and should be handled in the hood. Hydrogen peroxide, 30% (H_2O_2) [CAS 7722-84-1] is an oxidizer that can cause mild burns on skin. Care should be taken to avoid contact. In the event of direct contact, wash the affected area immediately with cool water.

Hydrochloric acid (HCl) [CAS 7647-01-0] and nitric acid (HNO_3) [CAS 7697-37-2] are strong acids that can cause severe burns on skin. Care should be taken to avoid contact. In the event of direct contact, wash the affected area immediately with copious amounts of cool water. Nitric acid is a strong oxidizer; contact with certain organic reagents may initiate strong exothermic reactions.

Glacial acetic acid ($\text{HC}_2\text{H}_3\text{O}_2$) [CAS 64-19-7] is a corrosive liquid with a strong odor. Contact with skin can cause burns and prolonged inhalation can cause lung tissue damage. In the event of contact, wash the affected area immediately with cool water. Glacial acetic acid should be handled in the hood.

Aqueous ammonia (NH_3) [CAS 7664-41-7] has a pungent, suffocating odor. Ammonia gas produced from the concentrated solution is extremely destructive to tissues of the mucous membranes

and upper respiratory tract. As with skin contact with any base, the solution produces a slippery sensation and can cause mild to severe burns unless washed off immediately.

Sodium nitrite (NaNO_2) [CAS 7632-00-0] is a stable salt, incompatible with strong oxidizing agents. The salt is used as a food preservative but should be considered toxic if swallowed.

Experimental Conditions. All chemicals were of reagent grade or better and were used as purchased without further purification. In all synthetic procedures, the cobalt(II) complex is formed first then oxidized to the cobalt(III) complex. All UV-visible spectra were recorded without delay after synthesis from 250 to 700 nm for the complexes as synthesized unless otherwise noted. Deionized water was used as the reference solution for all spectra.

Hexaaquacobalt(II) [$\text{Co}(\text{H}_2\text{O})_6$] $^{2+}$ stock solution. Dissolve 0.613 g of $\text{Co}(\text{NO}_3)_2 \cdot 6 \text{H}_2\text{O}$ (2.1 mmol) in 500 mL of deionized water to produce an approximately 0.0042 M stock solution. (Note that the UV-visible spectrum of this complex is not taken.)

Triglycinatocobalt(III) [$\text{Co}(\text{gly})_3$]. Add 0.75 g of sodium glycinate (*syn.* glycine, sodium salt) (7.7 mmol) to 10 mL of stock [$\text{Co}(\text{H}_2\text{O})_6$] $^{2+}$ solution. Add 5 mL of 3% hydrogen peroxide to oxidize the cobalt. Allow the reaction to proceed for approximately 5 min to completely form the purple complex.

Trioxalatocobaltate(III) [$\text{Co}(\text{ox})_3$] $^{3-}$. Add 1.55 g of $\text{K}_2\text{C}_2\text{O}_4 \cdot \text{H}_2\text{O}$ (8.4 mmol) to 10.0 mL of the stock [$\text{Co}(\text{H}_2\text{O})_6$] $^{2+}$ solution. Add 10 mL of 3% H_2O_2 to oxidize the metal and heat gently to 30 to 40 °C with stirring (10 to 15 min) until blue-green color is seen.

Tricarbonatocobaltate(III) [$\text{Co}(\text{CO}_3)_3$] $^{3-}$. Dissolve 2.99 g $\text{Co}(\text{NO}_3)_2 \cdot 6 \text{H}_2\text{O}$ (10.3 mmol) in a solution of 50 mL of water and 0.5 mL 30% H_2O_2 . Combine this solution all at once with a solution of 16.9 g NaHCO_3 (269 mmol) in 50 mL H_2O and 0.5 mL 30% H_2O_2 . Use a flask large enough to allow for rapid gas evolution and stir for approximately 1 min until bubbling stops. Dilute 1 mL of the resulting solution to 25 mL prior to obtaining the UV-visible spectrum. Save the remaining solution for the preparation of hexaaquacobalt(III), [$\text{Co}(\text{H}_2\text{O})_6$] $^{3+}$ [27].

Hexaaquacobalt(III) [$\text{Co}(\text{H}_2\text{O})_6$] $^{3+}$. Add 20 mL of the solution containing tricarbonatocobaltate(III) a few milliliters at a time to 80 mL of 4 M HNO_3 . Addition of the [$\text{Co}(\text{CO}_3)_3$] $^{3-}$ solution to the nitric acid should be slow enough to prevent bubbling over. Hydrochloric acid must be avoided because the cobalt(III) ion can be reduced by chloride ion. Obtain the UV-visible spectrum. Save this solution for the preparation of tris(1,10-phenanthroline)cobalt(III), [$\text{Co}(\text{phen})_3$] $^{3+}$.

Tris(1,10-phenanthroline)cobalt(III) [$\text{Co}(\text{phen})_3$] $^{3+}$. Add 0.115 g 1,10-phenanthroline (0.5 mmol) to 10 mL of the solution containing hexaaquacobalt(III). Add to this 10 mL of 3% H_2O_2 and stir for 5 min.

Hexanitrocobaltate(III) [$\text{Co}(\text{NO}_2)_6$] $^{3-}$. Dissolve 0.38 g $\text{Co}(\text{NO}_3)_2 \cdot 6 \text{H}_2\text{O}$ (1.31 mmol) in 3 mL of water. Dissolve 3.07 g NaNO_2 (44.5 mmol) in 5 mL of water. Combine the two solutions and add 1.5 mL glacial acetic acid. Note that the solution will bubble vigorously. Dilute to 50 mL, stopper, and shake vigorously for 2 to 3 min. Dilute 1 mL of the solution to 50 mL with water prior to recording the UV-visible spectrum.

Hexaamminecobalt(III) [$\text{Co}(\text{NH}_3)_6$] $^{3+}$. In a flask, dissolve 9.74 g $\text{Co}(\text{NO}_3)_2 \cdot 6 \text{H}_2\text{O}$ (33.5 mmol) and 5.33 g NH_4Cl (99.7 mmol) in 50 mL of water. Add 17 mL of concentrated aqueous ammonia and suspend 0.13 g activated charcoal in the solution. Vigorously bubble air through the solution with a fritted-glass gas-dispersion tube until oxidation is complete (approximately 3 to 4 hours). Bubbling with pure oxygen reduces the oxidation time to approximately 1 h. Isolate the resulting charcoal-contaminated precipitate by vacuum filtration using Whatman #1 (or other fine porosity) filter paper in a Büchner funnel. Dissolve the solid in 50 mL of 0.24 M HCl and heat gently for 10 min. Remove the activated charcoal from the hot solution by vacuum filtration in a Büchner funnel. Dilute 1 mL of the solution to 10 mL with water prior to recording the UV-visible spectrum.

Hexacyanocobaltate(III) [$\text{Co}(\text{CN})_6$] $^{3-}$. Add 2.55 g $\text{CoCl}_2 \cdot 6 \text{H}_2\text{O}$ (10.7 mmol) to approximately 75 mL of water and bring to a boil. With stirring, add a solution of 1.56 g (23.9 mmol) KCN in 30 mL

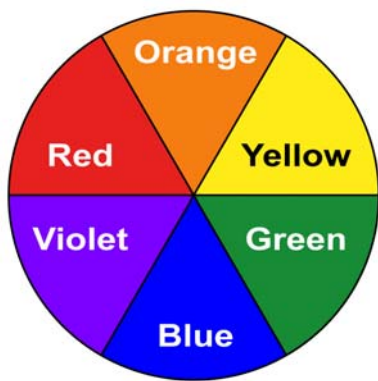


Figure 1. Transmission color wheel used for the qualitative ranking of ligands based on their perceived color. Solutions will display the color opposite the wavelength absorbed; therefore, yellow solutions, which correspond to an absorption in the violet/ultraviolet region, represent those complexes with the largest Δ_0 , and green solutions, which correspond to absorptions in the red/infrared regions, represent complexes with smaller Δ_0 values.



Figure 2. Photograph of solutions produced in the current experiment. Solutions are ordered according to the ligand spectrochemical series: (a) CN^- , (b) NO_2^- , (c) phen, (d) en, (e) NH_3 , (f) gly, (g) H_2O , (h) ox^{2-} , (i) CO_3^{2-} .

water by pipette to the solution. This results in a red/brown colored solution. Separate the purple solid by vacuum filtration and wash the solid with ice-cold water. Add the still-moist solid to 2.99 g KCN (45.9 mmol) in 50 mL H_2O and heat to boiling. Conversion from the green cobalt(II) to yellow cobalt(III)–cyanide complex will be observed. After the yellow color is formed record UV–visible spectrum. The solution must be analyzed warm to prevent conversion to the Co(II)–cyanide complex.

Tris(ethylenediamine)cobalt(III) $[\text{Co}(\text{en})_3]^{3+}$. Very slowly add 6.81 mL ethylenediamine to 4.1 mL of 6 M HCl. Combine this mixture with 2.95 g $\text{Co}(\text{NO}_3)_2 \cdot 6 \text{H}_2\text{O}$ (10.1 mmol) in a round-bottom flask and dissolve with 20 mL H_2O . Vigorously bubble air through the solution with a fritted-glass gas-dispersion tube until oxidation is complete (approximately 3 to 4 h). Bubbling with pure oxygen reduces the oxidation time to approximately 1 h. Place the round-bottom flask in a steam bath until most of the volume has decreased and a distinct layer of solid forms on the top of the solution. Filter the solution and wash with ethanol until the washings are clear. Dry the yellow/orange crystals in the oven. Dissolve a very small sample (approximately 0.02g) in 10 mL of water and observe the UV–visible spectrum.

Alternately, the solution is prepared as above; however, before placing on a steam bath, stir vigorously and add ethanol until solid just

forms. Then, add the same amount again of ethanol to facilitate precipitation. Filter the resulting solid and wash with cold ethanol. Dissolve a very small sample (approximately 0.02g) in 10 mL of water and observe the UV–visible spectrum.

Results and Discussion

Analysis. Analysis and ranking of the ligands into the spectrochemical series can be done at three different levels. The most basic level involves ranking the ligands by the color of the cobalt compound they produce. This qualitative ranking of ligands is appropriate for the high school level and is accomplished using the color transmission wheel in Figure 1. Solutions will display the color opposite the wavelength absorbed. This method of ranking ligands is valid given the direct correlation of the wavelength of light absorbed to the energy of the electron transition in the molecule (Δ_0).

For the introductory college chemistry level where UV–visible spectrophotometers are available, ligands can be quantitatively ranked based on the lowest energy wavelengths of maximum absorption (λ_{max}). The λ_{max} of lowest energy can be used to generate the spectrochemical series, as it is directly proportional to, though not equal to, Δ_0 .

For high-spin d^6 Co(III) complexes, two $e_g \leftarrow t_{2g}$ transitions are seen in the UV–visible region due to the fact that half of the of the six possible orbital changes (for example $d_{z^2} \leftarrow d_{xz}$) give rise to orbital transitions that result in a net increase in electron–electron repulsion. Note that other spin-forbidden transitions are possible but have such low probability that the associated molar absorptivities are negligible. In addition, ligand-to-metal charge transfer bands (LMCT) are seen in the ultraviolet region in almost all cases, but do not provide information about metal d orbitals and need not be considered in the present analysis.

For more advanced college chemistry courses, true values for Δ_0 are calculated using Tanabe–Sugano diagrams as described below. In addition, in classes in which metal-to-ligand bonding interactions are discussed in detail, the spectrochemical series not only can be produced, but the ranking of ligands can be justified/explained in terms of ligand-bonding interactions, such as σ and π -acceptor/donor.

Discussion. Figure 2 shows a photograph of colored solutions produced in this experiment. The solutions are qualitatively arranged by color using the transmission color wheel in Figure 1. Yellow solutions, which correspond to an absorption in the violet/ultraviolet region, represent those complexes with the largest Δ_0 . Green solutions, which correspond to absorptions in the red/infrared regions, represent complexes with smaller Δ_0 values.

Figure 3 shows example spectra for four of the complexes produced in the experiment. The relevant spectroscopic data are summarized in Table 1. Using only the lowest energy (longest wavelength) λ_{max} for each complex and arranging the complexes in order of highest-to-lowest energy (corresponding to highest-to-lowest Δ_0), the spectrochemical series produced is



where phen = 1,10-phenanthroline, en = ethylenediamine, gly = glycine, and ox^{2-} = oxalate. This experimentally-derived series is almost identical to literature-published spectrochemical series [28–32], except for a reversal at H_2O and ox^{2-} , although

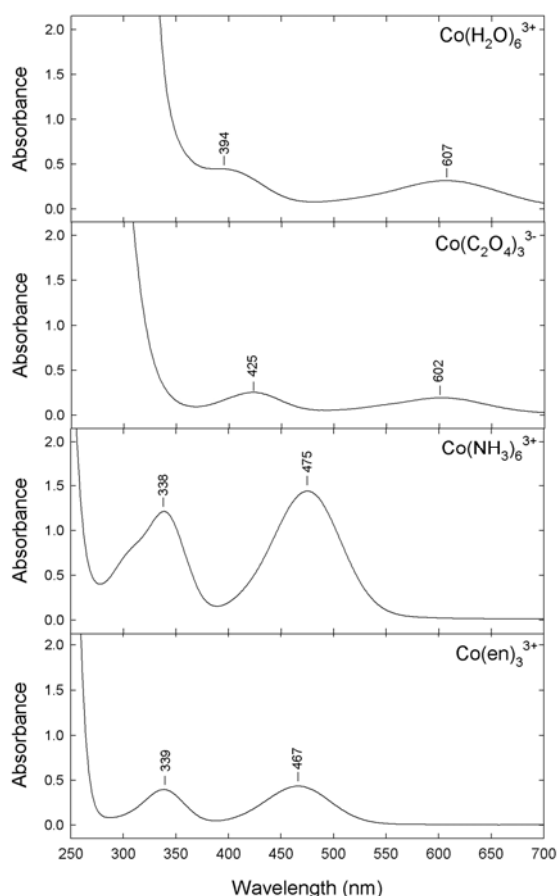


Figure 3. Representative spectra obtained for high spin d^6 Co(III) complexes two $e_g \leftarrow t_{2g}$ transitions are seen in the UV-visible region due to the fact that half of the of the six possible orbital changes (for example $d_{z^2} \leftarrow d_{xz}$) give rise to orbital transitions that result in a net increase in electron–electron repulsion.

Table 1. Student Data and Calculations Necessary for Determining Δ_0 (See text for details)

Ligand	Complex color	λ_{\max_1} ^a	λ_{\max_2} ^a	E/B ^b	B ^c	Δ_0/B ^d	Δ_0 ^e
CN ⁻	pale	256	309	92.2	350.8	96.67	33909
	yellow	(39063)	(32362)	6			
NO ₂ ⁻	light	290	365	62.4	438.7	66.11	29004
	yellow	(34483)	(27397)	5			
phen	yellow	273	451	16.4	1347	19.44	26198
		(36630)	(22173)	6			
en	dark	339	467	35.8	596.9	38.89	23214
	yellow	(29499)	(21413)	7			
NH ₃	orange	339	475	33.1	635.0	36.11	22931
		(29499)	(21053)	5			
gly	purple	382	538	32.6	570.0	35.56	20266
		(26178)	(18587)	1			
H ₂ O	blue	394	607	23.4	709.4	26.11	18406
		(25381)	(16474)	2			
ox ²⁻	teal	425	602	30.9	531.7	33.89	18153
		(23529)	(16611)	8			
CO ₃ ²⁻	emerald	425	626	27.1	587.5	30.00	17624
	green	(23529)	(15974)	9			

^aUpper value in nm; wavenumbers in parenthesis. ^bObtained from the TS diagram using the ratio of high to low transition energies (see text). ^cRacah parameter in cm^{-1} calculated using the lower energy transition. ^dObtained from the TS diagram (see text). ^eCrystal field splitting energy in cm^{-1} .

it has been reported that the crystal field splitting parameters for H₂O and ox²⁻ are virtually identical [28].

Calculation of the ligand field splitting parameter Δ_0 was done using Tanabe–Sugano (TS) diagrams as per Huheey et al [33]. This is necessary as high spin d^6 Co(III) complexes give rise to two $e_g \leftarrow t_{2g}$ transitions in the UV–visible region because half of the of the six possible orbital changes result in a net increase in electron–electron repulsion. The $d_{z^2} \leftarrow d_{yz}$ transition involves promoting an electron already centered about the electron rich z axis (due to the occupied d_{xz} and d_{yz} orbitals). This does not result in a large net increase in electron–electron repulsion; however, the transition from $d_{z^2} \leftarrow d_{xy}$ involves promoting an electron from the non-electron-rich xy plane to the electron-rich z axis, resulting in a large increase in electron–electron repulsion. These transitions are therefore higher in energy.

The calculation of Δ_0 is accomplished as follows, using the oxalate complex as an example. The spectrum of $[\text{Co}(\text{ox})_3]^{3-}$ is shown in Figure 3; three peaks can be seen. The peaks at 602 nm and 425 nm correspond to the two $e_g \leftarrow t_{2g}$ transitions. These represent the ${}^1T_{1g} \leftarrow {}^1A_{1g}$ (lower energy) and ${}^1T_{2g} \leftarrow {}^1A_{1g}$ (higher energy) transitions. (The peak at 307 nm corresponds to a ligand-to-metal charge-transfer band (LMCT) and is not used in this analysis.) Traditionally, in most textbooks, the transition wavelengths are converted to energy, generally in wavenumbers, so this convention will be continued here. The ratio of the two transitions is calculated as follows:

$$\frac{23529 \text{ cm}^{-1}}{16611 \text{ cm}^{-1}} = 1.42$$

The Tanabe–Sugano diagram for d^6 complexes (Figure 4) is used to find the point along the x axis where the ratio of these two transition energies is equal to 1.42, which corresponds to a unitless Δ_0/B value of 35.00 (where B is the Racah parameter value for the coordinated metal). This point, for the lower-energy transition, corresponds on the E/B axis to a value of 32.03 (where E is the energy of the lower-energy transition).

The Racah parameter is easily calculated from the E/B value and lowest transition energy.

$$\frac{E}{B} = 32.03$$

$$E = 16611 \text{ cm}^{-1}$$

$$\therefore B = 518.7 \text{ cm}^{-1}$$

Alternatively, the higher transition energy may be used and (data not included) yields practically no difference in the results. Solving for Δ_0 ,

$$\frac{\Delta_0}{B} = 35.00$$

$$\therefore \Delta_0 = 18153 \text{ cm}^{-1}$$

This value is in excellent agreement with Jørgensen's [34] reported value of $18,020 \text{ cm}^{-1}$.

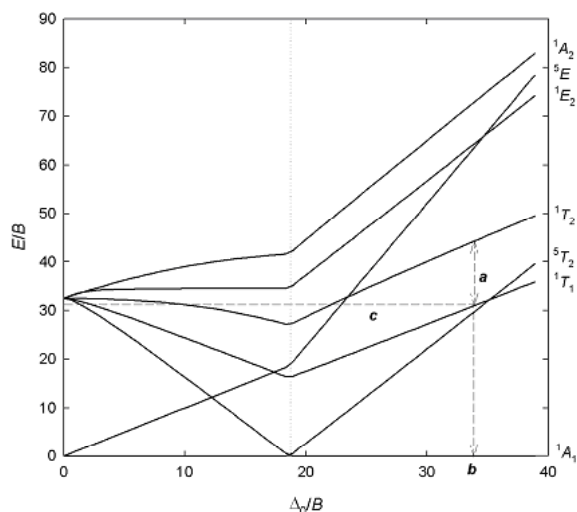


Figure 4. The Tanabe–Sugano diagram for allowed electronic transitions in the d^6 octahedral system. The dotted line at $\Delta_o/B = 18.9$ is the point at which the complex crosses from high-spin to low-spin. Dashed lines refer to the example in the text for $\text{Co}(\text{ox})_3^{3-}$. Line *a* is the point along the *x* axis (Δ_o/B) and *b* is where the ratio of UV–visible absorption energies is 1.42. Line *c* intercepts the value of E/B for the lowest energy transition used to calculate the Racah parameter.

It should be noted that the precision of this method is limited by students' ability to extract useful values from the Tanabe–Sugano diagrams as printed in textbooks. Generally, all TS diagrams presented in textbooks are impractical, being far too small and, for many complexes, extend insufficiently far along the Δ_o/B to reach the region of interest of many simple complexes. The present study has used more precise values obtained from tables developed by Professor Robert J. Lancashire of the University of West Indies [35]. A modified version of the table with only the relevant spin-allowed transitions for d^6 low-spin complexes is available (See supporting material).

Reevaluating the results using calculated crystal field splitting parameters yields an identical spectrochemical series as those found in the literature [28–32].

Further studies are being done to determine the pedagogical efficacy of the current experiment.

Acknowledgment. The authors would like to thank Pepperdine University Natural Science Division and the Seaver College Research Council for funding; Amit Gill, Natalie Aranda, Tiffany Asche, Mary Jones, and Scott Bolan for their assistance on this project; and Professor Robert J. Lancashire of the University of West Indies for his assistance with the Tanabe–Sugano diagrams.

Supporting Materials. An introduction to coordination compounds and crystal field theory and raw data for the octahedral d^6 Tanabe–Sugano diagram are included as supporting material in a Zip file (<http://dx.doi.org/10.1333/s00897050867a>)

References and Notes

1. Staver, J. R.; Halsted, D. A. *J. Res. Sci. Teach.* **1985**, *22*, 437–447.

2. Peterson, R. F.; Treagust, D. F. *J. Chem. Educ.* **1989**, *66*, 459–460.
3. Peterson, R. F.; Treagust, D. F.; Garnett, P. *J. Res. Sci. Teach.* **1989**, *26*, 301–314.
4. Bowen, C. W.; Bunce, D. M. *Chem. Educator* [online] **1997**, *2*, 1–17; DOI 10.1333/s00897970118a.
5. Ahtee, M.; Varjola, I. *Int. J. Sci. Educ.* **1998**, *20*, 305–316.
6. Boo, H. K. *J. Res. Sci. Teach.* **1998**, *35*, 569.
7. Taber, K. S. *Int. J. Sci. Educ.* **1998**, *20*, 597–608.
8. Birk, J. P.; Kurtz, M. J. *J. Chem. Educ.* **1999**, *76*, 124–128.
9. Rioux, F. *Chem. Educator* [online] **2001**, *6*, 288–290; DOI 10.1333/s00897010509a.
10. Zavitas, A. *J. Chem. Educ.* **2001**, *78*, 417.
11. Taagepera, M.; Arasasingham, R.; Potter, F.; Foroudi, A.; Lam, G., J. *Chem. Educ.* **2002**, *79*, 756.
12. Peacock-López, E. *Chem. Educator* [online] **2003**, *8*, 96–101; DOI 10.1333/s00897030676a.
13. Rioux, F. *Chem. Educator* [online] **2003**, *8*, 10–12; DOI 10.1333/s00897030650a.
14. Sinex, S.; Gage, B. *Chem. Educator* [online] **2003**, *8*, 266–270; DOI 10.1333/s00897030701a.
15. Trapp, C. Johnson, R. *J. Chem. Educ.* **1967**, *44*, 527.
16. Olson, G. *J. Chem. Educ.* **1969**, *46*, 508.
17. King, H. *J. Chem. Educ.* **1971**, *48*, 482.
18. Potts, R. A. *J. Chem. Educ.* **1974**, *51*, 539.
19. Shakhshiri, B.; Dirreen, G.; Juergens, J. *J. Chem. Educ.* **1980**, *57*, 900.
20. Williams, G.; Olmsted, J.; Breksa, A. *J. Chem. Educ.* **1989**, *66*, 1043.
21. Thomas, N.; Pringle, K.; Deacon, G. *J. Chem. Educ.* **1989**, *66*, 516–517.
22. Apel, E.; Ferguson, L.; Marshman, G.; Monks, R.; Sakurada, S.; Treballa, J. The Woodrow Wilson Leadership Program in Chemistry. <http://www.woodrow.org/teachers/chemistry/institutes/1986/exp35.html> (accessed Jan 2005).
23. Marsden, S. Chemistry Resources for Students and Teachers. <http://www.chemtopics.com/aplab/complexions.pdf> (accessed Jan 2005).
24. Brooks, L. <http://www.sonoma.edu/users/b/brooks/115b/complex.html> (accessed Jan 2005).
25. Szafran, Z.; Pik, R.; Singh. *Microscale Inorganic Chemistry*; Wiley & Sons: New York, 1991; pp 248–252.
26. Cotton, F. A.; Wilkinson, G. *Advanced Inorganic Chemistry*, 6th ed.; p 882; Schaffer, S.; Schaffer, C. *J. Chem. Educ.* **1996**, *73*, 180.
27. Modified from Schaffer, S. C.; Schaffer, C. E. *J. Chem. Educ.* **1996**, *73*, 180–181.
28. Jørgensen, C. K. *Adv. Chem. Phys.* **1963**, *5*, 65; Miessler, G. L.; Tarr, D. A. *Inorganic Chemistry*, 2nd ed.; Wiley-Interscience: New York; p 334.
29. Kiss, A.; Czegledy, D. *Z. Anorg. Allg. Chem.* **1938**, *235*, 407–426.
30. Mead, A. *Trans. Faraday Soc.* **1934**, *30*, 1052–1058.
31. Shimura, Y.; Tsuchida, T. *Bull. Chem. Soc. Jpn.* **1956**, *29*, 311–316.
32. Jørgensen, C. K. *Advances in Chemical Physics*, **1963**, *5*, 94–95.
33. Huheey, J. E., Keiter, E. A., Keiter, R. L. *Inorganic Chemistry*, 4th ed.; Benjamin Cummings: San Francisco, CA; pp 442–447.
34. Jørgensen, C. K. *Adv. Chem. Phys.* **1963**, *5*, 63.
35. <http://wwwchem.uwimona.edu/jm:1104/courses/Tanabe-Sugano/TSSpread.html> (accessed Jan 2005)